sustainability

Article

Optimal Operation of Low-Capacity Heat Pump Systems for Residential Buildings through Thermal Energy Storage

Alessandro Franco *, Carlo Bartoli, Paolo Conti and Daniele Testi

Department of Energy, Systems, Territory, and Constructions Engineering (DESTEC), University of Pisa, Largo Lucio Lazzarino, 56122 Pisa, Italy; carlo.bartoli@unipi.it (C.B.); paolo.conti@unipi.it (P.C.); daniele.testi@unipi.it (D.T.)

* Correspondence: alessandro.franco@ing.unipi.it

Abstract: The paper provides results from a hardware-in-the-loop experimental campaign on the operation of an air-source heat pump (HP) for heating a reference dwelling in Pisa, Italy. The system performances suffer from typical oversizing of heat emission devices and high water-supply temperature, resulting in HP inefficiencies, frequent on-off cycles, and relevant thermal losses on the hydronic loop. An experimentally validated HP model under different supply temperatures and part-load conditions is used to simulate the installation of a thermal storage between heat generator and emitters, in both series and parallel arrangements. Results relative to a typical residential apartment show that the presence of the thermal storage in series configuration ensures smoother heat pump operation and energy performance improvement. The number of daily on-off cycles can be reduced from 40 to 10, also saving one-third of electric energy with the same building loads. Preliminary guidelines are proposed for correctly sizing the tank in relation to the HP capacity and the average daily heating load of the building. A storage volume of about 70 L for each kilowatt of nominal heating capacity is suggested.

Keywords: buildings; energy efficiency; heat pumps (HP); hardware-in-the-loop (HiL); thermal energy storage (TES); optimal control

Citation: Franco, A.; Bartoli, C.; Conti, P.; Testi, D. Optimal Operation of Low-Capacity Heat Pump Systems for Residential Buildings through Thermal Energy Storage. *Sustainability* **2021**, *13*, 7200. https://doi.org/10.3390/su13137200

Academic Editor: Manosh C. Paul

Received: 26 May 2021
Accepted: 24 June 2021
Published: 27 June 2021

1. Introduction

The control of heating, ventilation, and air conditioning (HVAC) systems in residential or public buildings for optimal energy efficiency is widely considered in the current literature, and it is often connected with the objective of indoor air quality, as largely discussed by the authors in a recent paper in [1].

Heat pump (HP) systems are a strategic technology to increase the efficiency of heat generation and the penetration of electricity produced with renewable energy systems in buildings, as discussed in some recent papers [2–4]. Moreover, HPs are a relevant element in smart microgrids and nearly Zero Energy Buildings (nZEB), adding flexibility to the system and allowing shifts in energy demand from heat to electricity and from fossil fuels to renewables [5,6].

As a drawback, HP efficiency is significantly reduced at partial-load and intermittent operation, caused by frequent start and stop cycles, mainly during mid-seasons.

The coupling of a thermal energy storage (TES) with a HP is a key to improve the performance of the heating system, also implementing appropriate control strategies. The addition of a TES can be particularly useful to increase the penetration of renewable energy in the heating sector, favoring self-consumption of electricity by operating the HP, as discussed in [7,8].

The use of TES for the optimal operation of energy systems is analyzed in recent publications [9,10]. However, fully established criteria for optimal sizing and control of heat pumps coupled to thermal storages are not yet available. A quite advanced approach is model predictive control, as discussed in [11–13], even though its application requires accurate forecasting capabilities and nonnegligible computational effort.

Another critical aspect for an optimal synthesis, sizing, and operation of such systems is the sensitivity of their performance to dynamically varying loads caused by the variation of climatic conditions, such as external temperature and relative humidity. Simulation models should always be refined by experimental measurements; to this aim some emerging techniques are available today, such as the "hardware-in-the-loop" (HiL) experimentation methodology. The general elements of this approach can be found in [14–18].

With a HiL system it is possible to conduct tests on heat pumps or in general on heating, ventilation, and air conditioning systems with ad hoc emulators of building loads. With this approach, the economic effort and the time needed to develop accurate performance models are greatly reduced, and simulation and optimization activities can be performed in a context of reliability of the obtained results.

In the above framework, this paper moves from the experimental data collected on the performance of an air-to-water heat pump coupled with the emulated heating system of a dwelling in the mild climate of Pisa, Italy [19], analyzing the role of thermal storage tanks coupled with the heat pump to optimize the system operation and reduce the energy consumption compared to conventional direct heating.

The experimental data reported in [19] are obtained on a system without thermal storage and clearly show the performance deterioration of the heat pump under frequent part-load and on-off regimes, motivating the present study. In fact, we will evaluate the advantages and criticalities of introducing a thermal storage between the heat pump and the heat emission devices.

Thanks to the coupling of a TES in series or in parallel configuration, the HP operation is expected to become smoother and improve the operative performance, reducing the total energy consumption, even if heat losses from the thermal storage and higher water supply temperatures could counteract the energy efficiency gains.

Simulations of the system subject to the experimental loads will be performed using a "hardware-in-the-loop" system. The effect of the water tank volume in relation to the heat pump capacity and daily thermal load will also be analyzed, with the aim of providing useful criteria and guidelines, joined with sizing indications for designers of these integrated configurations.

In short, the novelty of this paper compared to the current state of the art lies in the following aspects, explored in the next sections: (i) the use of an innovative methodology based on hardware-in-the-loop experimental tests coupled with dynamic simulations of the building and heating system; (ii) the investigation on the role in terms of energy efficiency of a series-connected storage in heat pump systems; (iii) the proposal of a handy criterion of optimal storage sizing.

2. Definition of the Research Problem

2.1. Analysis of the Real Operation of Heat Pumps and Performance Indexes

As explained above, the systematic use of HP technology represents today a promising way for increasing energy efficiency, only if the HP is properly sized and operated. The HP system performance can be highly reduced under many circumstances, such as high temperature lift, defrost operation, partial loads, and frequent on-off cycles. Some of these conditions occur when the HP must match variable heating demands in response to the building thermal dynamics or during mid-season or in quite temperate climatic conditions, as the Mediterranean ones.

Besides the conventional Coefficient of Performance (COP), additional indexes can be defined to appropriately compare different operational modes of the same HP systems:

- COP_{nom}, or nominal full-load COP provided by the HP manufacturer at the reference sources temperature, in accordance with technical standards (e.g., EN 14511-2:2018 [20]). For instance, the reference temperature values for air-to-water heat pumps are 7 °C and 35 °C for outdoor air and supply water temperature, respectively;

- COP_{DC}, the full-load performances provided by the HP manufacturer at the different external and supply temperatures provided by technical standards (e.g., EN 14511-2:2018 [20] and EN 14825:2018 [21]). The data on these datasheets are generally marked with the subscript DC that indicates a quantity evaluated at maximum compressor speed;
- COP_{HP}, or the HP operative part-load COP, experimentally measured or simulated through a validated HP model. This index accounts for both external and supply temperatures, together with the effects of the capacity control;
- COP_{sys}, or the HP overall system performance, calculated as the ratio between the heat provided to the building by the emission system, $\dot{Q}_u$, and the electric input used by the HP, $\dot{W}_{HP,in}$. This value considers not only the HP performance but also all the thermal losses in the other pieces of equipment (e.g., pipework, thermal inertial storages, or puffers);
- η^{II}_{DC}, or the second-law or exergy efficiency of the HP unit. This index is based on the manufacturers' experimental COP_{DC} values, considering the reference supply and outdoor temperature $T_{out,HP,DC}$ and $T_{a,in,HP,DC}$ (see Equation (1)):

$$\eta^{\mathrm{II}}_{\mathrm{DC}} = \mathrm{COP}_{\mathrm{DC}} \frac{\mathrm{T}_{\mathrm{out,HP,DC}} - \mathrm{T}_{\mathrm{a,in,HP,DC}}}{\mathrm{T}_{\mathrm{out,HP,DC}} + 273.15} \quad (1)$$

A common HP performance evaluation methodology consists of interpolating the η^{II}_{DC} depending on actual operative temperatures.

The just-mentioned indexes refer to the instantaneous thermal or electrical power exchanged by the HP unit or system. However, it is also interesting to analyze their average value over a reference period, τ (e.g., a month, a year, a season). Some of the most common time-integral coefficients of performance are:

- $SCOP$, or Seasonal Coefficient of Performance, defined as the ratio between the thermal energy output and electrical energy input of the HP device ($SCOP_{HP}$) or the overall HP system ($SCOP_{sys}$) over the considered period τ (see Equations (2) and (3)):

$$SCOP_{HP} = \frac{\int_\tau \dot{Q}_{HP}\, d\tau}{\int_\tau \dot{W}_{HP,in} d\tau} = \frac{\int_\tau \dot{m}_{HP} c_f (T_{HP,out} - T_{HP,in}) d\tau}{\int_\tau \dot{W}_{HP,in} d\tau} = \frac{Q_{HP}}{W_{HP,in}} \quad (2)$$

$$SCOP_{sys} = \frac{\int_\tau \dot{Q}_u d\tau}{\int_\tau \dot{W}_{HP,in} d\tau} = \frac{Q_u}{W_{HP,in}} \quad (3)$$

- CR, or capacity ratio, is another interesting parameter associated with the real operation of the HP unit or system. It can be evaluated according to the delivered heat, Q, and the maximum available energy output at the nominal full-load power at the given external and supply temperatures over the considered time (off periods included):

$$CR = \frac{Q_{HP}}{\int_\tau \dot{Q}_{DC}(T_{out,HP}; T_{a,in,HP}) d\tau} \quad (4)$$

According to the above-mentioned technical standards, it is possible to evaluate a penalization factor, f_{CR}, as a function of CR, assuming values between 0 and 1.

Finally, the coefficient of performance of the HP, COP_{HP}, and the corresponding energy input, $W_{HP,in}$, can be evaluated as:

$$COP(T_{out,HP}; T_{a,in,HP}; CR) = \frac{T_{out,HP} + 273.15}{T_{out,HP} - T_{a,in,HP}} * \eta^{II}_{DC} * \ f_{CR} \quad (5)$$

$$W_{HP,in} = \frac{Q_{HP}}{COP(T_{out,HP}; T_{a,in,HP}; CR)} \quad (6)$$

The COP values as defined in Equation (5) can be generally applied on an hourly, daily, or monthly time step, when proper f_{CR} expressions are available (see, for instance, EN 14825:2018 [21]).

A quite recent paper about the integration of photovoltaic (PV) plants and HP [2] proved that an oversized HP heating a residential building in Pisa, Italy, had a measured seasonal coefficient of performance ($SCOP_{sys}$) around 2, half of the nominal declared value of the COP_{nom} of the installed HP. This was caused by a very intermittent operation (i.e., low CR values), mainly during the mid-season period (February, March, and November), when the operation of the HP is limited to only some hours (not above four) during the day, due to the quite high average outside temperature.

A similar problem has been evidenced by other authors in different climatic conditions and areas. Even when the system is correctly sized, Dongellini and Morini in [22] showed that on-off cycling losses are responsible for a penalty in the $SCOP_{HP}$ of an air-to-water HP as high as 12%, when coupled to a multi-family house located in Bolzano, Italy.

Higher penalty values, around 18%, were measured by Piechurski et al. in [23] for an air-source HP working under partial load and serving an office building in Wrocław, Poland; in addition, energy efficiency reductions up to 30% were observed for very short operating cycles (less than 10 min). Similarly, Bagarella et al. in [24] obtained penalizations exceeding 12% due to cycling losses of an air-to-water HP coupled to a single-family house located in Padua, Italy; in this case, the inclusion of a TES was also simulated, and the influence of the water tank volume on the HP system energy performance was analyzed, finding an optimal sizing at about 50 L per kilowatt of HP capacity.

2.2. The Integration of Heat Pump and Thermal Energy Storage

All the above-described experimental and simulation works show how the performance of HPs can be significantly penalized by on-off and part-load operation or, in any case, by working conditions different from a stable and stationary regime, typical of cold and hot climatic conditions, as reported in manufacturers' datasheet and technical standards. This explains the increasing attention devoted to TES integrated in HP systems, which have the purpose of decoupling the heat produced by the HP from the one required by the building, guaranteeing a smoother HP operation, lower peaks of the generated thermal power, and higher energy efficiency, as discussed in [25–27].

The performance of a heating system consisting of an HP with an integrated storage tank has been evaluated in the last years by several authors, by means of direct experimental analysis, as in [28], or by means of theoretical analysis and Computational Fluid Dynamics (CFD) calculations, as in [29], but the results proposed are only limited to quite specific applications.

The storage system appears to be functional for protecting the lifetime of the heat generation unit, and particularly of its compressor, whose life is reduced by a too-high number of on-off cycles. A further advantage of avoiding intermittencies is represented by the possibility of obtaining improved thermal comfort inside the building. Furthermore, a proper storage reduces the variations of indoor air temperature during the HP cycle reversals executed by the device for defrosting the evaporator heat exchanger. A comprehensive review on HP systems with TES for heating of buildings is presented by Osterman and Stritih in [30].

Another issue involving TES is their position in the hydraulic loop, which can be either in series between the HP device and the building emission system (a passive tank), as effectively implemented in [31], or in a parallel arrangement (the so-called active storage), as in the experimental research by Meng et al. [32].

The connection in series adds thermal inertia to the hydronic loop, with direct peak shaving and valley filling of the heating load; on-off cycles are effectively reduced, and heat losses are limited. On the other hand, the configuration in parallel with a by-pass path allows for predictive control of the storage temperature level for planning an efficient energy dispatch, also based on the operation of other integrated components; in this case, the system flexibility is improved [10], but the increased storage heat losses and the higher supply temperature needed from the HP for thermal energy charging are drawbacks to be carefully considered in the system analysis.

In order to provide some quantitative results for the optimal design and integration of heat pumps and thermal storages, we have applied a hybrid experimental and numerical approach that combines hardware-in-the-loop tests and dynamic simulations to a specific building system, as explained in the next section.

3. Test and Simulation Methodology

This section discusses the integration of a hydronic thermal storage tank into the system in heating mode and its effects on the performance of the heat pump. It was decided to broaden the analysis on this integrated system to reduce the on-off cycles of the HP and the consequent thermal losses and seek optimal operation and high performance of the HP, compared to the configuration of direct coupling with the building.

The proposed procedure follows this sequence of operations:

- run of experimental tests on a "hardware-in-the-loop" apparatus, emulating the dynamics of a selected building under real climatic conditions and with different control strategies of the heat generation unit;
- validation of the models of the heating system components according to the experimental data (baseline case);
- identification of alternative layouts of the heating system (in our case, integrating a TES in different hydraulic configurations) and simulation of its energy performance under the same climate and loads of the baseline case, to appreciate the role of the TES and for optimization purposes.

The characteristics of the experimental facility, the conditions of the tests conducted on the baseline HP system, and the models and layouts implemented in the simulations of the TES-integrated systems are given in the next sub-sections.

3.1. Description of the Hardware-in-the-Loop Apparatus

The demonstrator through which the experimental campaign was carried out is positioned in the DESTEC laboratory of the University of Pisa. It is composed of various thermal and electrical devices: some of them are real physical parts of the system, others act as emulators. The experimental setup consists of two plant sections:

- The generating section, consisting of the systems that generate and store thermal energy: an air–water electrically driven heat pump (with a scroll compressor, plate heat exchangers, and R-134a as working fluid), and a hot storage tank. The latter device acts as generator during the "discharging" phase: to this aim, the storage is equipped with a heat exchanging coil connected with the user section;
- The user section, which emulates the energy performance of a building and of its heat emission system. It consists of an external heat sink, a plate exchanger, a mixing valve, and a circulator dynamically controlled in real-time through a dynamic energy simulation routine. The hot storage can also act as user device during its "charging" phase: in this case, the fluid coming from the heat generator is directly pumped into the bulk volume.

The junction point between the generating and user sections is represented by the plate heat exchanger. The size of the experimental apparatus is tailored to the typical design thermal load of a single-family home. The water content of the primary circuit also corresponds to the typical volume of a residential heating system, around 45 L. This volume also includes two inertial vessels, containing a total mass of water of about 15 kg each, installed on the return branch of the HP-generating section to ensure a configuration closer to the real case and improving the performance of the HP, reducing the effects of transients on the circuit. Figure 1 shows the system diagram of the DESTEC demonstrator, including all its components and sensors for data acquisition, with a particular focus on the heat pump, in particular an air–water heat pump, the storage system, and the building emulator. Table 1 reports the characteristics of the installed thermal storage tank. A more detailed analysis of the system was provided by the authors of the present paper in a previous publication [19].

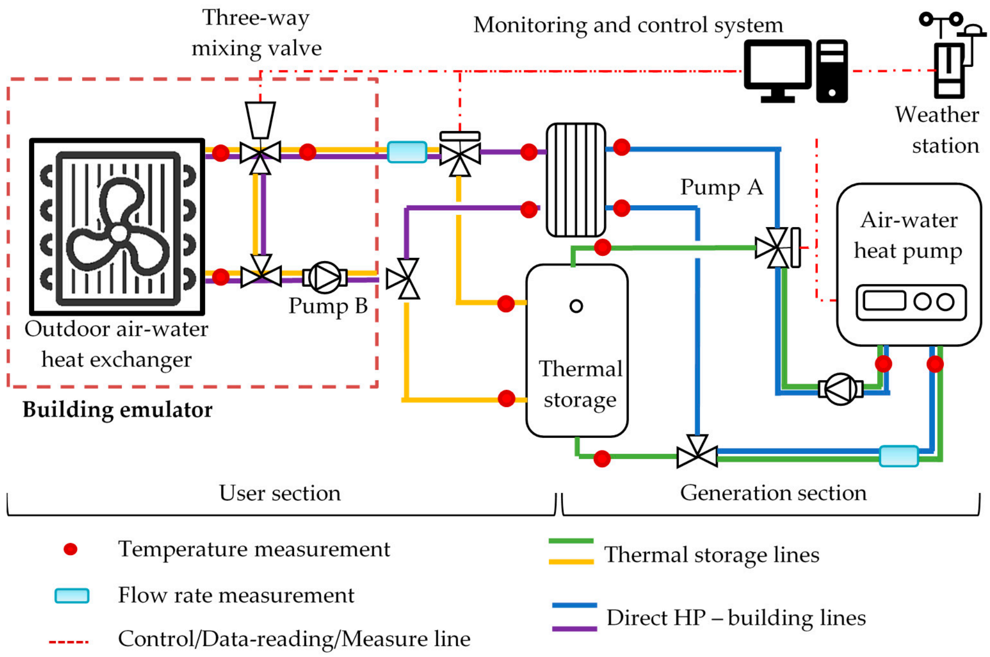

Figure 1. Schematic of the DESTEC hardware-in-the-loop apparatus.

Table 1. Characteristics of the thermal storage tanks.

Variable	Value
Volume of the water tank	520 L
Heat loss coefficient	1.5 W/K
Nominal heat transfer coefficient of the primary coil	670 W/(m^{2}K)
Heat exchange area of the coil	4.5 m^2

3.2. Tests Performed on the Baseline Configuration

The baseline configuration corresponds to the experimental setup and reference building described in [19], with the HP directly serving the building load, without a TES. Details on the measurement system and on its accuracy are given in Appendix A.

The served building (a typical apartment built in the 1980s of 84 m^2 floor area) is emulated according to the validated dynamic model reported in the next subsection. The building is situated in Pisa (1694 Heating Degree Day). Reference outdoor climate data are presented in Table 2, reported by CTI in [33].

Table 2. Reference climatic data for Pisa.

	Jan	Feb	Mar	Apr	May	Jun	Jul	Aug	Sep	Oct	Nov	Dec	Year
Outdoor temperature (°C)	7.3	7.4	10.7	12.9	17.9	20.6	22.9	23.1	19.8	15.6	11.7	7.6	14.8
Irradiation on horizontal surface (kWh/(m^2 d))	1.6	2.3	3.3	4.3	5.9	6.4	6.8	5.9	4.4	2.6	1.9	1.4	3.9
Outdoor relative humidity (%)	85.0	74.8	79.8	78.9	74.4	74.2	71.5	76.6	81.5	86.2	78.3	85.8	79.0
Wind velocity (m/s)	1.8	1.5	1.3	1.6	1.9	1.6	1.7	1.3	1.0	1.4	1.6	2.1	1.6

The experimental activity was performed during the heating period, considering different operating conditions; in this section, we present the results of two test periods, with different climate and system control conditions, as shown in Table 3.

Table 3. Test periods and conditions.

Test Period and Conditions	Setpoint Temperature	Avg. External Temperature	Water Supply Temperature	Fan Coil Speed
TP1	20 °C	8.7 °C	40 °C	Intermediate
TP2	20 °C	11.5 °C	35 °C	Low

In the first test period (TP1, from 20 December 2019 to 13 January 2020), representing typical winter conditions and in general the coldest period of the year, the system is controlled with standard values of water supply temperature and fan coil speed. In the second test period (TP2, from 24 January 2020, to 12 February 2020), which is warmer than the first one and is representative of a typical mid-season condition (typical average temperature of March or November), both parameters were lowered, to better match the reduced heat load.

3.3. Models for the Simulation of the Building and Storage-Integrated Systems and Layouts

The experimental analysis on the HiL system requires an accurate energy model of the building to run the building emulator (BE). For defining the model of the BE, a classical thermal network approach can be used, as suggested in technical standards as EN ISO 52016-1:2017 [34]) or in some commercial software. In this model, the building elements can be considered as electrical nodes connected to each other by equivalent electrical resistances, capacities, time-dependent current, and voltage generators. In this way, if N is the number of thermal nodes considered in the model, including the one of indoor air, the building dynamic model corresponds to a ($N \times N$) linear set of equations that can be quickly solved at each time step. The evolution of nodal temperature is a function of climate data (e.g., outdoor air temperature, solar irradiance, sky temperature), heat gains (linked to the presence of people inside the building, the miscellaneous electrical appliances, and the lighting systems), and heat exchanged by the system terminals. All these elements can be modeled as voltage or current generators: their source value is updated at each time step, according to a given profile (e.g., occupants' presence) or measured quantities in the HiL apparatus (e.g., climate data and supply temperature to the heat emission systems). The heat gain delivered by the emission system, which is relevant in this specific application, can be evaluated through a few additional linear equations to be added to the overall set representing the building. In this work, we use fan coil units (FCUs) as heat terminal units.

To simulate the effects of a storage-integrated system, a validated model of the examined HP pump system is employed to evaluate the HP performance under the same climate and building energy demand profiles described with TP1 and TP2 in Table 3. Details on this model are given in Appendix B.

The series-connected and parallel-connected storage arrangements in the HP system layout are illustrated in Figure 2. To evaluate the performance of the HP unit and of the overall HP system, the following parameters, already defined in Section 2.1, are considered: HP capacity ratio, CR, defined by Equation (2); COP_{nom}, COP_{HP}, and COP_{sys}.

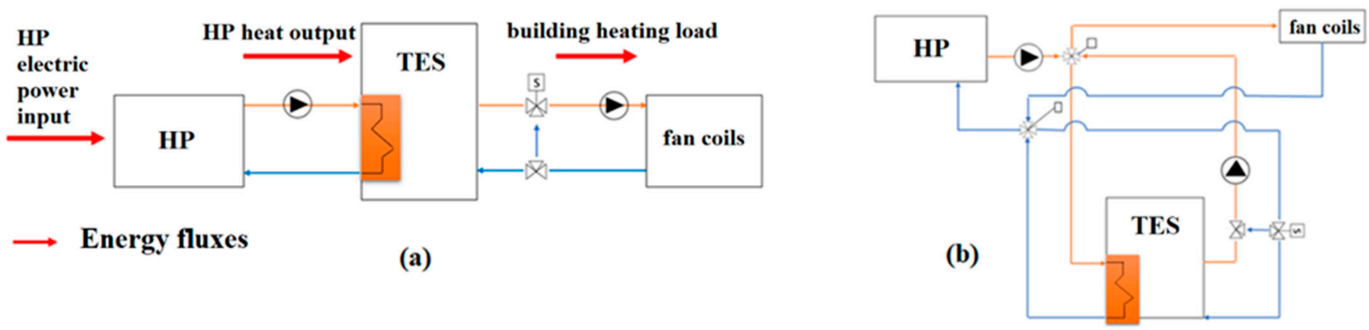

Figure 2. Schematic of the heat pump system with the series-connected (**a**) and parallel-connected (**b**) storage.

4. Results and Discussion

The above-described HiL apparatus was used to emulate the seasonal winter performance of a commercial AHP acting as heat generator in the selected building. Three cases are analyzed: the baseline case of operation, in which only HP is considered, and two cases in which a storage system in serial configuration and the last one with storage in parallel are considered to better regulate the operation of the HP.

In the final part of this section, some general considerations about the sizing of the storage system to optimize the operation of the HP will be proposed.

4.1. Experimental Results of the Baseline Case without Storage

Analyzing the experimental system performance, an important difference emerges in terms of heat pump operation between the two test periods, as reported in Table 3. TP1 shows an average of 39 on-off cycles per day (average duration of the on period: about half an hour) versus only 2–3 cycles per day in TP2 (average duration of the on period: almost 4 h). This happens even though the lower external temperature of TP1 should favor a more continuous operation of the HP; hence, the effect can be attributed to the higher values of supply temperature and heat emitted by the fan coil units, which in common practice tend to be oversized due to conservative design approaches. As a matter of fact, a small variation in these control parameters can produce dramatic consequences for HP dynamics, thermal losses on the hydraulic loop (particularly relevant during the off periods), and overall system performance, which are very difficult to predict a priori. This observation suggests that the addition of a TES could be highly beneficial when the system operates in TP1 conditions, and it could lead to improved system robustness and overall increased performance.

In Figure 3a, the experimental values of COP_{HP} during TP1 and TP2 are compared to the nominal values of the HP as a function of the external air temperature, T_{ext}. As expected, and coherently with the results of Table 4, the COP part-load penalization is higher during TP2, due to the lower CR values. However, as shown in Figure 3b, the overall system performance is significantly lower during the coldest period TP1, owing to the lower duration of on periods (only 26 min as average value) and subsequent thermal losses associated with the on-off cycles.

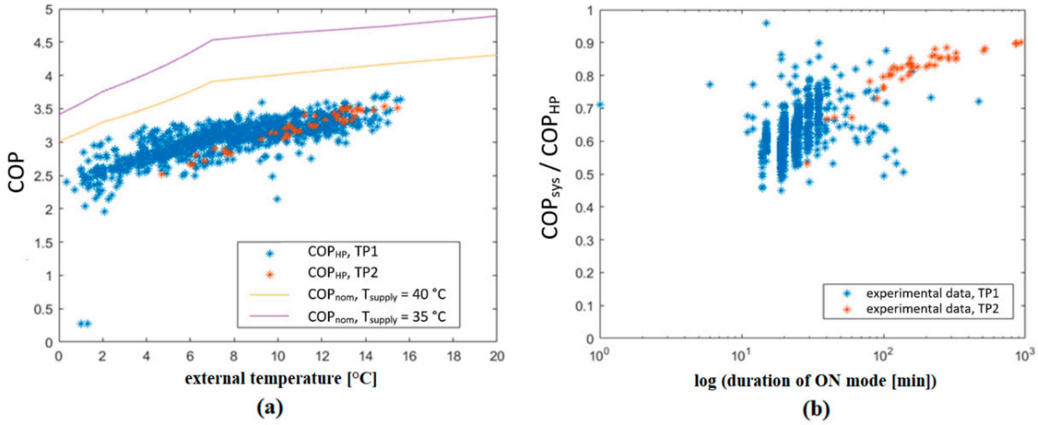

Figure 3. Experimental heat pump performance during the two operating phases TP1 and TP2: COP_{nom} vs. COP_{HP} as a (**a**) and experimental system performance during TP1 and TP2 as a function of the duration of the on period (**b**).

Table 4. Experimental results for the baseline configuration.

Test Conditions	TP1	TP2
Number of on-off cycles per day	39	2–3
Average duration of the single on period (min)	26	234
Average CR	0.66	0.33
Average COP_{nom}	4.37	4.86
Average COP_{HP}	3.03	3.20
Average COP_{sys}	1.95	2.61
Input electric energy per heating degree day (kWh/HDD)	1.90	0.71

These latter inefficiencies prevail against the ones due to part-load operation, and higher electric energy input is recorded in TP1. The effect cannot be ascribable to the longer duration and colder temperatures of TP1, because the electric energy uses reported in Table 3 are scaled in terms of heating degree days (HDD), defined with reference to the internal setpoint temperature. Figure 4 provides experimental heat pump performance COP_HP as a function of outdoor air temperature, supply water temperature and capacity ratio: four different conditions are analyzed. For all the cases the real experimental curve (identified with the point) and the smoothed one (identified with minus sign) are represented.

As shown in Figure 4, for the present case study, the direct use of the HP would be in general not satisfactory, because the COP at partial-load conditions, defined by reduced value of CR, appears to be much lower than the declared values, referring to well-defined design parameters, as a function of supply water temperature, $T_{out,HP}$, outdoor air temperature, $T_{a,in,HP}$, and capacity ratio CR, represented by the green curve.

From the analysis of the experimental tests performed without a storage system, we can conclude that a TES could mitigate the negative effects of inefficient system operation, particularly under TP1 conditions. Hence, its inclusion in series and parallel configuration will be evaluated by dedicated simulations under the same test conditions.

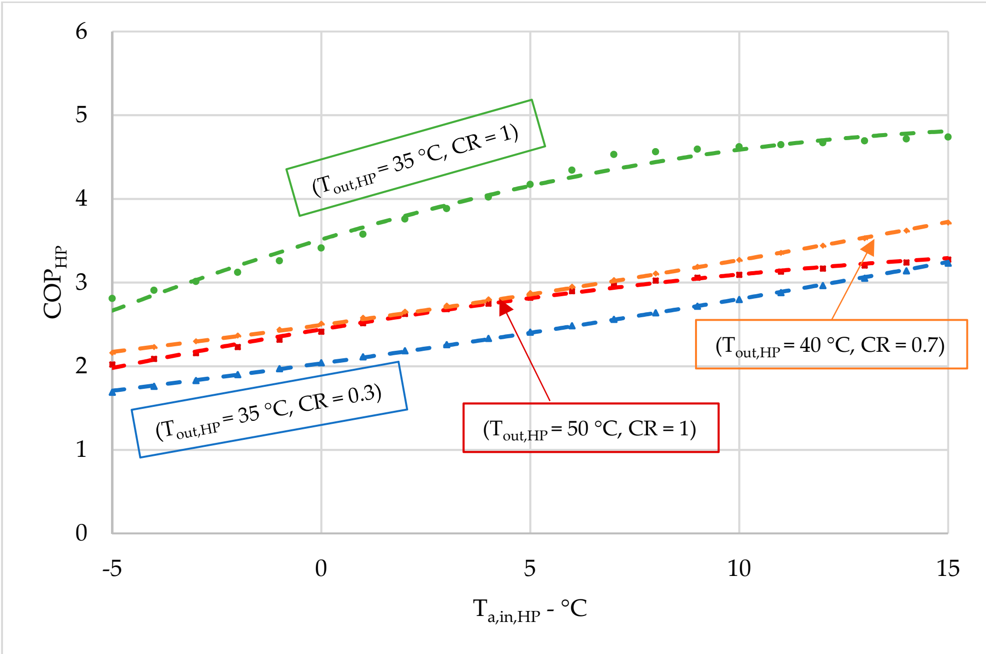

Figure 4. Experimental heat pump performance COP_{HP} as a function of outdoor air temperature, supply water temperature and capacity ratio.

4.2. Simulation Results of the Series-Connected Storage

The storage-integrated layout of Figure 2a was simulated by means of the HP and TES models defined in Section 3.3. The main benefit of the series configuration is the high HP capacity ratio at which heat could be generated compared to the baseline configuration (illustrated in Section 4.1). On the contrary, HP supply temperature, $T_{out,HP}$, must be higher to allow the heat transfer within the thermal storage coil. Moreover, the tank introduces additional thermal losses through its insulation. Finally, the viability of the series configuration depends on the relevance of these opposing phenomena on the operational $SCOP_{sys}$. As previously mentioned, the energy performance simulations were conducted under the same climatic conditions and thermal loads of the experimental baseline. This was done for comparison purposes, and it is a necessary constraint for achieving the final objective of correctly sizing the tank. The obtained results are reported in Table 4. The thermal flywheel effect introduced by the additional inertia of the passive storage is helpful in greatly reducing the number of on-off cycles in TP1, stabilizing the system performance. The operative capacity ratios are close to 1 both in TP1 and TP2, with negligible penalizations on the nominal COP_{HP} values. The electric energy uses per heating degree day are highly reduced in TP1 and slightly increased in TP2 (to appreciate the differences, it is possible to compare the data of Tables 4 and 5). However, we emphasize the system improvement in this layout, which not only performs at a higher energy efficiency but can also limit the effects of unfavorable operative conditions caused by oversized heat emission devices or inappropriate control settings: on-off cycles would affect the end-user loop without directly reducing the HP coefficient of performance.

Table 5. Numerical results for the series-connected storage configuration under TP1 and TP2 conditions.

Test Conditions	TP1	TP2
Number of on-off cycles per day	11	4
Average duration of each on period (min)	75	59
Average CR	0.98	0.97
Average COP_{nom}	3.15	3.27
Average COP_{HP}	3.08	3.18
Average COP_{sys}	2.36	2.34
Input electric energy per heating degree day (kWh/HDD)	1.27	0.77

Prior to searching further improvements by optimizing the tank size (the outcomes of this activity will be shown in Section 4.4), we evaluated the arrangement with the parallel-connected storage. These latter results are discussed in the next section.

4.3. Simulation Results of the Parallel-Connected Storage

The purpose of this configuration is to introduce additional flexibility with respect to the series configuration: the system can theoretically switch between the baseline and series configurations, choosing the optimal one according to the actual operative conditions. Again, the simulations were performed under the same climate and loads of the baseline. Despite the expectations, the simulation results on this specific system are unsatisfactory. In any case, the system performance is impaired, mainly due to the higher HP supply temperature (compensating the mentioned expected advantages on COP_{HP}) and the increased thermal losses on the loop and especially on the storage, kept at a higher temperature. These results suggest that a reward from the active storage configuration could be expected only if advanced model predictive control techniques are applied, as in [35], or in system layouts with a greater degree of integration, for instance, when solar thermal collectors aid to raise the TES temperature, as in Yin et al. [36], or in an electric market scenario with dynamically varying energy prices, as in Patteeuw at al. [37].

4.4. Analysis of the Results and Proposal of a Sizing Rule for the Thermal Energy Storage System

Focusing on the passive storage configuration and aiming at providing general guidelines for the sizing of the accumulation tank in a heating system, two methodologies are proposed. The first rule is very straightforward, providing the suggested ratio between TES liters of water (L) and design heating power (kW). Following the simulations, this value can be approximately considered in 70 L for each kW installed. The obtained results show that the size of the storage tank for obtaining optimal operation of the HP is of the same order of magnitude but a little higher than the size suggested in a similar study provided in [24].

The second method is instead more comprehensive and finds the storage capacity based on the average daily thermal energy uses. Here the objective is sizing the tank to guarantee an appropriate duration of each "on period" (for example, at least 2 h per each on cycle).

Figure 5 shows the trend of the calculated volume as a function of the daily heating load. It is interesting to note how the curve initially increases and then decreases: it increases to provide additional inertia when the load increases, and it decreases to avoid unnecessary thermal losses at higher loads. Thus, according to the exposed results, an optimal value of the storage unit can be evaluated considering the power of the HP.

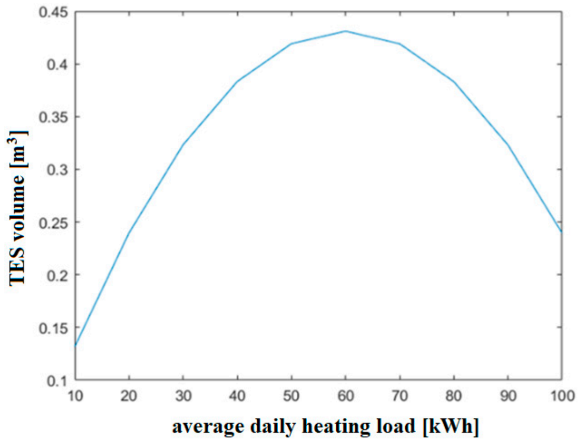

Figure 5. Thermal storage capacity as a function of the average daily load of the heating system.

5. Conclusions and Future Works

The paper proceeds from a "hardware-in-the-loop" (HiL) experimental campaign with the purpose of evaluating the positive effect of the use of thermal energy storage system for increasing the operational efficiency of a HP system.

In particular, the operation of an air-to-water heat pump heating a reference residential apartment in Pisa has been analyzed comparing the differences in two operational modes in a basic configuration and using a thermal energy storage system.

In the basic configuration without energy storage, the system performances suffer from typical oversizing of heat emission units and high water-supply temperature, resulting in HP inefficiencies, frequent on-off cycles, and relevant thermal losses on the hydronic loop—this causes a relevant reduction of the seasonal performance COP with respect to the typical value diffused by the HP manufacturers.

Using an experimentally validated HP model under different supply temperatures and part-load conditions, the installation of a TES between generator and emitters is simulated in both series and parallel arrangements.

Results confirm that the presence of a series-connected TES ensures smoother HP operation and energy performance improvement. In particular, the use of a TES is relevant if the external temperature is quite low (less than 10 °C), and the HP supply temperature and emission system controls are consequently set to provide greater heating power. In this case, a TES in series configuration has proven to be ideal for mitigating the losses due to numerous and short on-off cycles and increase the duration of the on periods for the HP. In particular, the number of on-off cycles is reduced from about 40 per day to about 10 per day and a 33% electric energy saving is obtained. The same positive results are not obtained in milder winter conditions, and the contribution of the TES cannot be appreciated. Furthermore, the appropriate size of the TES was shown, to obtain a proper duration of the HP on period, around 2 h.

Concerning the possibility of furnishing a direct sizing rule, a general criterion, considering typical residential building configuration a storage volume of about 70 L for each kW of nominal heating capacity is required.

The results of this activity are here limited to a specific case, but they can be used to extrapolate general considerations about the utilization of TES for optimization of HP operation in civil buildings. With this perspective, it will be important to carry out additional experimental work to validate the accumulation model (perfectly mixed storage) and, if this aspect emerges as critical, replace it with a more accurate one (stratified storage). Moreover, as future work it would be interesting to evaluate the benefits of the application of the same strategy using innovative HP operating with more eco-friendly refrigerants.

Author Contributions: Conceptualization, A.F. and D.T.; methodology, A.F., P.C. and D.T.; software, A.F., P.C. and D.T.; validation, A.F. and D.T.; formal analysis, A.F., C.B., P.C. and D.T.; investigation,

P.C.; resources, A.F., C.B., P.C. and D.T.; data curation, A.F. and D.T.; writing—original draft preparation, A.F. and D.T.; writing—review and editing, A.F., C.B., P.C. and D.T.; supervision, A.F., C.B., P.C. and D.T.; funding acquisition, A.F., D.T. All authors have read and agreed to the published version of the manuscript.

Funding: The authors gratefully acknowledge the financial support of the Italian Ministry of Education, University and Research (MIUR), in the framework of the Research Project of Relevant National Interest (PRIN) "The energy FLEXibility of enhanced HEAT pumps for the next generation of sustainable buildings (FLEXHEAT)" (PRIN 2017, Sector PE8, Line A, Grant n. 33).

Institutional Review Board Statement: Not applicable.

Informed Consent Statement: Not applicable.

Data Availability Statement: The data presented in this study are available on request from the corresponding author.

Acknowledgments: The authors gratefully acknowledge the financial support of the Italian Ministry of Education, University and Research (MIUR), in the framework of the Research Project of Relevant National Interest (PRIN), "The energy FLEXibility of enhanced HEAT pumps for the next generation of sustainable buildings (FLEXHEAT)" (PRIN 2017, Sector PE8, Line A, Grant n. 33). We also wish to thank Selene Paladini for running, during her Master Thesis, several experimental tests and numerical simulations.

Conflicts of Interest: The authors declare no conflict of interest.

Nomenclature

Acronyms	
AHP	Air-to-water heat pump
BE	Building emulator
CFD	Computational Fluid Dynamics
FCU	Fan coil unit
HiL	Hardware-in-the-loop system
HDD	Heating degree days
HP	Heat pump
HVAC	Heating, ventilation, and air Conditioning
nZEB	net Zero Energy Building
TES	Thermal energy storage
ZEB	Zero Energy Building
Symbols	
COP	coefficient of performance
CR	capacity ratio
c	specific heat, $J/(kg\ K)$
f	penalization factor
Q	thermal energy used, kWh
$\dot{Q}$	thermal power, W
$SCOP$	mean or Seasonal Coefficient of Performance
T	Temperature, $^{\circ}C$ or K
$\dot{W}$	electrical power, W
W	electrical energy used, kWh
η^{II}	Second law efficiency
τ	operational time, s
Subscripts	
a	air
ext	external air
CR	referred to the capacity ratio
DC	declared by the manufacturer
f	fluid
i	indoor air

in	inlet or input
non	nominal value
out	outlet or output
r	return
s	supply
sys	of the whole system

Appendix A. Accuracy of the Measurement System

The experimental apparatus uses industrial measurement equipment, accepting its typical accuracy. Laboratory instruments are excluded, because we intend to develop control strategies to be implemented in already existing systems, using their typical measurement, control, and actuation devices.

Temperature is measured by 11 Negative Temperature Coefficient (NTC) thermistors. NTC thermistors were selected for their accuracy in the operational temperature range of the HiL apparatus and for their simple installation compared to thermocouples. The NTC has been previously calibrated, showing an accuracy in the $-5 \div 50$ °C range of ± 0.2 K (with 95% confidence level, i.e., 2σ). The corresponding accuracy on a temperature difference measurement is ± 0.3. K. For measuring the water temperature, the NTC thermistors were inserted in a submerged copper probe, reaching the middle of the flow section. Flow rates are measured by Kármán vortex flowmeters, located as shown in Figure 2. The accuracy after calibration in the $5 \div 25$ L/m range is ± 0.0225 L/m (with 95% confidence level).

The accuracy on thermal power, which is obtained as the product of mass flow rate, specific heat and temperature difference, was evaluated by error propagation theory, from the partial derivative of thermal power with respect to each of the dependent variables, according to the methodology described in [38]. Around the nominal flow rate (980 L/h) and temperature difference (5 K), the error is about 320 W, corresponding to a relative error of 5.5% (the nominal AHP capacity is 5.8 kW).

The weather station was placed on the roof of the laboratory building. Table A1 reports the accuracy of its instruments.

Table A1. Accuracy of the weather station components.

Sensor	Measured Quantity	Accuracy
Thermistor (PT 100)	Dry bulb temperature (°C)	± 0.15 K $\pm$ 0.1%
Metal oxide's electrical capacity	Relative humidity $(0 \div 1)$	$\pm 0.015 \pm 1.5\%$
Piezoresistive pressure sensor	Air pressure (Pa)	± 50 Pa
Ultrasonic anemometer	Direction and speed (m/s)	$\pm 1°$ (direction) ± 0.2 m/s $\pm$ 2% reading (speed)
Thermopile pyranometer	Global solar irradiance $(\mathrm{W/m^2})$ in the $0.30 \div 2.80$ μm wavelength range	$\pm 10\%$
Thermopile pyrgeometer	Infrared sky radiation $(\mathrm{W/m^2})$ in the $5.5 \div 45$ μm wavelength range	$\pm 10\%$

Appendix B. Integrated System Modelling

To simulate the effects of a storage-integrated system, a validated model of the examined HP pump system was employed to evaluate the HP performance under the same climate and building energy demand profile of TP1 and TP2. Details are given in the current section.

The considered HP system is made of four main components: the heat pump generator, the thermal storage, the end-user loop (heat emitters included), and the generation loop (see Figure 2). The evolution of the overall system is simulated with a timestep of 1 min through the concurred solving of Equations (A1)–(A11).

Heat pump: the HP coefficient of performance is evaluated at each time step as a function of supply water temperature, $T_{out,HP}$, outdoor air temperature, $T_{a,in,HP}$, and capacity ratio CR. First, the full-load coefficient of performance, COP_{DC}, is evaluated through the interpolation of the manufacturer datasheet, depending on sources temperature. Then, the actual COP_{HP} at partial-load conditions are evaluated through the following formula:

$$COP_{HP} = COP_{DC}(T_{a,in,HP}, T_{out,HP}) \times f_{CR}(T_{out,HP}; T_{a,in,HP}; CR) \tag{A1}$$

where:

$$\begin{aligned} &f_{CR}(T_{out,HP}; T_{a,in,HP}; CR) = \\ &= \begin{cases} \mathrm{P}(T_{out,HP}; T_{a,in,HP}; CR), & CR < 0.75 \\ \mathrm{P}(T_{out,HP}; T_{a,in,HP}; 0.75) + \frac{1-\mathrm{P}(T_{out,HP}; T_{a,in,HP}; 0.75)}{1-0.75}(CR - 0.75), & CR \geq 0.75 \end{cases} \end{aligned} \tag{A2}$$

and:

$$\begin{aligned} &\mathrm{P}(T_{out,HP}; T_{a,in,HP}; CR) \\ &\qquad = c_1 + c_2 \times TR + c_3 \times TR^2 + c_4 \times TR \times CR + c_5 \times CR + c_6 \times CR^2 \\ &\qquad TR = \frac{T_{out,HP} + 273.15}{T_{a,in,HP} + 273.15} \qquad CR = \frac{\dot{Q}_{HP}}{\dot{Q}_{DC}(T^*_{out,HP}; T_{a,in,HP})} \\ &c_1 = 68.14 \quad c_2 = -151.50 \quad c_3 = 84.6 \quad c_4 = -4.66 \quad c_5 = 5.52 \quad c_6 = -1.06 \end{aligned} \tag{A3}$$

The polynomial coefficients in Equation (A3) are evaluated through a regression analysis of the data collected during the experimental phases TP1 and TP2. The average relative deviation between the experimental data and the model is about 5%.

The heat pump model also considers the maximum thermal power that can be delivered by the HP according to the temperature of the source, namely:

$$\dot{m}_{HP} c_w (T_{out,HP} - T_{in,HP}) = \min\left[\dot{m}_{HP} c_w \left(T^*_{out,HP} - T_{in,HP}\right); \dot{Q}_{DC}\left(T^*_{out,HP}; T_{a,in,HP}\right)\right] \tag{A4}$$

Thermal storage: the water tank is considered as a single thermal capacity, according to the classical perfectly mixed approach. The energy balance reads:

$$\rho_w c_w V_{TS} \frac{dT_{TS}}{dt} = \dot{Q}_{helix} - \dot{Q}_{user} - k_{l,TS}(T_{TS} - T_{amb,TS}) \tag{A5}$$

where V_{TS} is the tank volume, $\dot{Q}_{helix}$ is the thermal power delivered by the generation loop through the primary coil of the storage, $\dot{Q}_{user}$ is the thermal power delivered to the end-user loop (see Equation (A11)), $k_{l,TS}$ is the heat loss coefficient (see Table 1), $T_{amb,TS}$ is the ambient temperature where the thermal storage is located. The thermal power $\dot{Q}_{helix}$ is evaluated through the classical $\epsilon - NTU$ method for heat exchanger analysis [39], namely:

$$\dot{Q}_{helix} = \epsilon_{helix}\, \dot{m}_{HP} c_w (T_{helix,in} - T_{TS}) \tag{A6}$$

$$\epsilon_{helix} = 1 - \exp\left(-\frac{(UA)_{helix}}{\dot{m}_{HP} c_w}\right) \qquad (UA)_{helix} = (UA)_{helix,nom}\left(\frac{\overline{T_{helix}} - T_{TS}}{35}\right)^{0.25} \tag{A7}$$

$$T_{helix,out} = T_{helix,in} - \frac{\dot{Q}_{helix}}{\dot{m}_{HP} c_w} \tag{A8}$$

where $(UA)_{helix,nom}$ corresponds to the nominal value of the heat transfer coefficient of the coil (see Table 1) provided by the manufacturer at the nominal temperature difference of 35 K.

Generation loop: the generation loop connects the heat pump generator to the primary coil of the thermal storage. The model of this component is based on the actual generation section of the HiL apparatus (see Figure 1). The main water content and the heat losses surface are in the return section of the loop, in correspondence with the puffer volume.

Therefore, we have assumed as negligible the water content and the heat losses of the supply section.

$$T_{helix,in} \approx T_{out,HP} \tag{A9}$$

Equation (A9) is coherent with the temperature data collected in the experimental phases. The return section of the generation loop is assumed as an equivalent perfectly mixed node, corresponding to the sum of the puffer and ducts volume. The energy balance reads:

$$\begin{aligned}\rho_w c_w V_{gen,loop} \frac{dT_{gen,loop}}{dt} = \dot{m}_{HP} c_w \left(T_{helix,out} - T_{gen,loop} \right) - \\ (UA)_{gen,loop} \left(T_{gen,loop} - T_{amb,TS} \right)\end{aligned} \tag{A10}$$

The effective water content, $V_{gen,loop}$, and heat loss coefficient, $(UA)_{gen,loop}$, are estimated as equal to 30 L and 6 W/K, respectively.

End-user loop: for the sake of comparison, the $\dot{Q}_u$ profile is the one measured during the two HiL experimental periods. As we discuss in Section 3, the thermal losses of the end-user loop depend on both pipework insulation and control efficiency. Indeed, the characteristics of the control system determine the number of on/off cycles and related inefficiencies. An actual evaluation of the water loop dynamics would require an accurate integrated model for both the HVAC system and building. For our simulation purposes, we refer to the global distribution and control efficiency, η_{user}. The latter value was evaluated according to the data collected during the TP2 experimental campaign equal to 0.82. Shortly, $\dot{Q}_{user}$ profile in Equation (A5) can be evaluated through the simple expression:

$$\dot{Q}_{user} = \dot{Q}_u / \eta_{user} \tag{A11}$$

The series-connected and parallel-connected storage arrangements in the HP system layout are illustrated in Figure 2.

References

1. Franco, A.; Bartoli, C.; Conti, P.; Miserocchi, L.; Testi, D. Multi-Objective Optimization of HVAC Operation for Balancing Energy Use and Occupant Comfort in Educational Buildings. *Energies* **2021**, *14*, 2847. [CrossRef]
2. Franco, A.; Fantozzi, F. Experimental analysis of a self consumption strategy for residential building: The integration of PV system and geothermal heat pump. *Renew. Energy* **2016**, *86*, 1075–1085. [CrossRef]
3. Fischer, D.; Madani, H. On heat pumps in smart grids: A review. *Renew. Sustain. Energy Rev.* **2017**, *70*, 342–357. [CrossRef]
4. Testi, D.; Urbanucci, L.; Giola, C.; Schito, E.; Conti, P. Stochastic optimal integration of decentralized heat pumps in a smart thermal and electric micro-grid. *Energy Convers. Manag.* **2020**, *210*, 112734. [CrossRef]
5. Conti, P.; Lutzemberger, G.; Schito, E.; Poli, D.; Testi, D. Multi-objective optimization of off-grid hybrid renewable energy systems in buildings with prior design-variable screening. *Energies* **2019**, *12*, 3026. [CrossRef]
6. Péan, T.Q.; Salom, J.; Costa-Castelló, R. Review of control strategies for improving the energy flexibility provided by heat pump systems in buildings. *J. Process. Control.* **2019**, *74*, 35–49. [CrossRef]
7. Mathiesen, B.V.; Lund, H.; Karlsson, K. 100% Renewable energy systems, climate mitigation and economic growth. *Appl. Energy* **2011**, *88*, 488–501. [CrossRef]
8. Franco, A.; Salza, P. Strategies for optimal penetration of intermittent renewables in complex energy systems based on techno-operational objectives. *Renew. Energy* **2011**, *36*, 743–753. [CrossRef]
9. Lund, P.D.; Lindgren, J.; Mikkola, J.; Salpakari, J. Review of energy system flexibility measures to enable high levels of variable renewable electricity. *Renew. Sustain. Energy Rev.* **2015**, *45*, 785–807. [CrossRef]
10. Reynders, G.; Lopes, R.A.; Marszal-Pomianowska, A.; Aelenei, D.; Martins, J.; Saelens, D. Energy flexible buildings: An evaluation of definitions and quantification methodologies applied to thermal storage. *Energy Build.* **2018**, *166*, 372–390. [CrossRef]
11. Arteconi, A.; Hewitt, N.J.; Polonara, F. Domestic demand-side management (DSM): Role of heat pumps and thermal energy storage (TES) systems. *Appl. Therm. Eng.* **2013**, *51*, 155–165. [CrossRef]
12. Beck, T.; Kondziella, H.; Huard, G.; Bruckner, T. Optimal operation, configuration and sizing of generation and storage technologies for residential heat pump systems in the spotlight of self-consumption of photovoltaic electricity. *Appl. Energy* **2017**, *188*, 604–619. [CrossRef]
13. Bianchini, G.; Casini, M.; Pepe, D.; Vicino, A.; Zanvettor, G.G. An integrated model predictive control approach for optimal HVAC and energy storage operation in large-scale buildings. *Appl. Energy* **2019**, *240*, 327–340. [CrossRef]

14. Bianchi, M.; Shafai, E.; Federal, S.; Geering, H.P. Comparing New Control Concepts for Heat Pump Heating Systems on a Test Bench with the Capability of House and Earth Probe Emulation. In Proceedings of the 8th International Energy Agency Heat Pump Conference, Las Vegas, NV, USA, 30 May–2 June 2005; pp. 1–11.
15. Fischer, D.; Wirtz, T.; Zerbe, K.D.; Wille-Haussmann, B.; Madani, H. Test Cases for Hardware in the Loop Testing of Air to Water Heat Pump Systems in a Smart Grid Context. In Proceedings of the International Congress of Refrigeration (ICR), Yokohama, Japan, 16–22 August 2015; pp. 3666–3673.
16. Stutterecker, W.; Schoberer, T.; Steindl, G. Development of a Hardware-in-the-Loop Test Method for Heat Pumps and Chillers. In Proceedings of the REHVA Annual Conference "Advanced HVAC and Natural Gas Technologies", Riga, Latvia, 6–9 May 2015; p. 117.
17. Frison, L.; Kleinstück, M.; Engelmann, P. Model-predictive control for testing energy flexible heat pump operation within a hardware-in-the-loop setting. *J. Phys. Conf. Ser.* **2019**, *1343*, 012068. [CrossRef]
18. Mehrfeld, P.; Nürenberg, M.; Knorr, M.; Schinke, L.; Beyer, M.; Grimm, M.; Lauster, M.; Müller, D.; Seifert, J.; Stergiaropoulos, K. Dynamic evaluations of heat pump and micro combined heat and power systems using the hardware-in-the-loop approach. *J. Build. Eng.* **2020**, *28*, 101032. [CrossRef]
19. Conti, P.; Bartoli, C.; Franco, A.; Testi, D. Experimental analysis of an air heat pump for heating service using a "hardware-in-the-loop" system. *Energies* **2020**, *13*, 4498. [CrossRef]
20. EN 14511–2. *Air Conditioners, Liquid Chilling Packages and Heat Pumps for Space Heating and Cooling and Process. Chillers, with Electrically Driven Compressors-Part. 2: Test. Conditions*; European Committee for Standardization (CEN): Brussels, Belgium, 2018.
21. EN 14825. *Air Conditioners, Liquid Chilling Packages and Heat Pumps, with Electrically Driven Compressors, for Space Heating and Cooling. Testing and Rating at Part. Load Conditions and Calculation of Seasonal Performance*; European Committee for Standardization (CEN): Brussels, Belgium, 2018.
22. Dongellini, M.; Morini, G.L. On-off Cycling Losses of Reversible Air-to-Water Heat Pump Systems as a Function of the Unit Power Modulation Capacity. *Energy Convers. Manag.* **2019**, *196*, 966–978. [CrossRef]
23. Piechurski, K.; Szulgowska-Zgrzywa, M.; Danielewicz, J. The impact of the work under partial load on the energy efficiency of an air-to-water heat pump. *E3S Web Conf.* **2017**, *17*, 00072. [CrossRef]
24. Bagarella, G.; Lazzarin, R.; Noro, M. Sizing strategy of on-off and modulating heat pump systems based on annual energy analysis. *Int. J. Refrig.* **2016**, *65*, 183–193. [CrossRef]
25. Pardo, N.; Montero, A.; Urchueguia, J.F. Optimization of hybrid–ground coupled and air source–heat pump systems in combination with thermal storage. *Appl. Therm. Eng.* **2010**, *30*, 1073–1077. [CrossRef]
26. Baeten, B.; Helsen, L.; Roigiers, F. Reduction of heat pump induced peak electricity use and required generation capacity through thermal energy storage and demand response. *Appl. Energy* **2017**, *195*, 184–195. [CrossRef]
27. Wang, Z.; Wang, F.; Li, G.; Song, M.; Ma, Z.; Ren, H.; Li, K. Experimental investigation on thermal characteristics of transcritical CO2 heat pump unit combined with thermal energy storage for residential heating. *Appl. Therm. Eng.* **2020**, *165*, 114505. [CrossRef]
28. Qu, M.; Lu, M.; Li, Z.; Song, X.; Chen, J.; Ziviani, D.; Braun, J.E. Thermal energy storage based (TES-based) reverse cycle defrosting control strategy optimization for a cascade air source heat pump. *Energy Build.* **2020**, *219*, 110014. [CrossRef]
29. Sifnaios, J.; Fan, J.; Olsen, L.; Madsen, C.; Furbo, S. Optimization of the coefficient of performance of a heat pump with an integrated storage tank–A computational fluid dynamics study. *Appl. Therm. Eng.* **2019**, *160*, 114014. [CrossRef]
30. Osterman, E.; Stritih, U. Review on compression heat pump systems with thermal energy storage for heating and cooling of buildings. *J. Energy Storage* **2021**, *39*, 102569. [CrossRef]
31. Renaldi, R.; Kiprakis, A.; Friedrich, D. An optimisation framework for thermal energy storage integration in a residential heat pump heating system. *Appl. Energy* **2017**, *186*, 520–529. [CrossRef]
32. Meng, Q.; Ren, X.; Wang, W.; Xiong, C.; Li, Y.; Xi, Y.; Yang, L. Reduction in on-off operations of an air source heat pump with active thermal storage and demand response: An experimental case study. *J. Energy Storage* **2021**, *36*, 102401. [CrossRef]
33. CTI (Italian Thermotechnical Committee). Italian Typical Meteorological Years. 2016. Available online: https://www.cti2000.it/index.php?controller=news&action=show&newsid=34985 (accessed on 10 May 2021).
34. EN 52016–1. *Energy Performance of Buildings-Energy Needs for Heating and Cooling, Internal Temperatures and Sensible and Latent Heat Loads-Part. 1: Calculation Procedures*; European Committee for Standardization (CEN): Brussels, Belgium, 2017.
35. D'Ettorre, F.; Conti, P.; Schito, E.; Testi, D. Model predictive control of a hybrid heat pump system and impact of the prediction horizon on cost-saving potential and optimal storage capacity. *Appl. Therm. Eng.* **2019**, *148*, 524–535. [CrossRef]
36. Yin, Z.; Enshen, L.; Xinhui, Z.; Zhenghao, J.; Qinjian, L.; Fei, L.; Yang, M. Combined solar heating and air-source heat pump system with energy storage: Thermal performance analysis and optimization. *Procedia Eng.* **2017**, *205*, 4090–4097. [CrossRef]
37. Patteeuw, D.; Bruninx, K.; Arteconi, A.; Delarue, E.; D'haeseleer, W.; Helsen, L. Integrated modeling of active demand response with electric heating systems coupled to thermal energy storage systems. *Appl. Energy* **2015**, *151*, 306–319. [CrossRef]
38. Moffat, R.J. Describing the Uncertainties in Experimental Results. *Exp. Therm. Fluid Sci.* **1988**, *1*, 3–17. [CrossRef]
39. Shah, R.K.; Sekulic, D.P. *Fundamentals of Heat Exchanger Design*; John Wiley and Sons: Hoborken, NJ, USA, 2003.